Algorithms for Tracking Interfaces in CFD and Material Science

J.A. Sethian *
Department of Mathematics
and
Lawrence Berkeley Laboratory

University of California
Berkeley, California 94720

Abstract

We describe new applications of the level set approach for following the evolution of complex interfaces. This approach is based on solving an initial value partial differential equation for a propagating level set function, using techniques borrowed from hyperbolic conservation laws. Topological changes, corner and cusp development, and accurate determination of geometric properties such as curvature and normal direction are naturally obtained in this setting. In this paper, we review some recent work, including fast level set methods, extensions to multiple fluid interfaces, generation of complex interior and exterior body-fitted grids, and applications to problems in combustion and material science.

1 Introduction

In this paper, we review some recent work which extends the capabilities of level set methods for tracking the evolution of complex interfaces, and summarize some new recent applications of these techniques. Level set methods, introduced by Osher and Sethian [25], offer highly robust and accurate methods for tracking interfaces moving under complex motions. Their major virtue is that they naturally construct the fundamental weak solution to surface propagation posed by Sethian [27, 28]. They work in any number of space dimensions, handle topological merging and breaking naturally, and are easy to program. They approximate the equations of motion for the underlying propagating surface, which resemble Hamilton-Jacobi equations with parabolic right-hand sides. The central mathematical idea is to view the moving front as a particular level set of a higher dimensional function. In this setting, sharp gradients and cusps can form easily, and the effects of curvature may be easily incorporated. The key numerical idea is to borrow the technology from the numerical solution of hyperbolic conservation laws and transfer these ideas to the Hamilton-Jacobi setting, which then guarantees that the correct entropy satisfying solution will be obtained.

*Supported in part by the Applied Mathematics Subprogram of the Office of Energy Research under contract DE-AC03-76SF00098, and the National Science Foundation and DARPA under grant DMS-8919074.

A variety of numerical algorithms are available to advance propagating interfaces in such areas as CFD, dendritic growth and solidification, flame/combustion models, and material processing. Roughly speaking, they fall into three general categories:

- *Marker/String Methods:* In these methods, a discrete parameterized version of the interface boundary is used. In two dimensions, marker particles are used; in three dimensions, a nodal triangularization of the interface is often developed. The positions of the nodes are then updated by determining front information about the normals and curvature from the marker representation. Such representations can be quite accurate, however, limitations exist for complex motions. To begin, if corners and cusps develop in the evolving front, markers usually form "swallowtail" solutions which must be removed through delooping techniques which attempt to enforce an entropy condition inherent in such motion (see [28]). Second, topological changes are difficult to handle; when regions merge, some markers must be removed. Third, significant instabilities in the front can result, since the underlying marker particle motions represent a weakly ill-posed initial value problem (see [25]). Finally, extensions of such methods to three dimensions require additional work.

- *Cell-Based Methods:* In these methods, the computational domain is divided into a set of cells which contain "volume fractions" These volume fractions are numbers between 0 and 1, and represent the fraction of each cell containing the physical material. At any time, the front can be reconstructed from these volume fractions. Advantages of such techniques include the ability to easily handle topological changes, adaptive mesh methods, and extensions to three dimensions. However, determination of geometric quantities such as normals and curvature can be inaccurate.

- *Characteristic Methods:* In these methods, "ray-trace"-like techniques are used. The characteristic equations for the propagating interface are used, and the entropy condition at forming corners (see [28]) is formally enforced by constructing the envelope of the evolving characteristics. Such methods handle the looping problems more naturally, but may be complex in three-dimensions and require adaptive adding and removing rays, which can cause instabilities and/or oversmoothing.

As discussed above, level set methods are powerful techniques for tracking interfaces that naturally handle corners and cusps that develop, correctly develop the correct weak solution that invokes the entropy condition introduced in [28], and extend in a straightforward manner to three dimensions. Since their introduction, in [25], the level set approach has been used in a wide collection of problems involving moving interfaces. Some of these applications include the generation of minimal surfaces [10], singularities and geodesics in moving curves and surfaces in [12], flame propagation [26, 36], fluid interfaces [6, 9], crystal growth and dendritic solidification [33], detection of self-similar surfaces [11], etching, deposition and lithography [2, 3], and shape reconstruction [23]. Extensions of the basic technique include fast methods in [1] and methods for multiple fluid interfaces [34]. The fundamental Eulerian perspective presented by this approach has since been adopted in many theoretical analyses of mean curvature flow, see in particular [14, 8], and related work in [4, 13, 15, 16, 19, 21].

In this paper, we discuss some of these applications, and recent work which extends the level set method to increase its power and versatility. In particular, we review work on the development of fast methods, methods for multiple interfaces and triple points, and fast methods for reinitialization which may be required in some complex cases. In the applications domain, we discuss the implementation of the level set methods

for propagating interfaces applied to crystal growth, flame stability and propagation, grid generation, and microfabrication problems in etching, deposition, and photolithography.

2 Fundamentals of the Level Set Method: Numerical Algorithms for Propagating Fronts

The fundamental aspects of front propagation in our context can be illustrated as follows. Let $\gamma(0)$ be a smooth, closed initial curve in R^2, and let $\gamma(t)$ be the one–parameter family of curves generated by moving $\gamma(0)$ along its normal vector field with speed $F(K)$. Here, $F(K)$ is a given scalar function of the curvature K. Thus, $n \cdot x_t = F(K)$, where x is the position vector of the curve, t is time, and n is the unit normal to the curve. It can be shown that a curve collapsing under its curvature shrinks to a circle, see [17, 18, 20].

Consider a speed function of the form $1 - \epsilon K$, where ϵ is a constant. An evolution equation for the curvature K, see [28], is given by

$$K_t = \epsilon K_{\alpha\alpha} + \epsilon K^3 - K^2 \tag{1}$$

where we have taken the second derivative of the curvature K with respect to arclength α. This is a reaction-diffusion equation; the drive toward singularities due to the reaction term $(\epsilon K^3 - K^2)$ is balanced by the smoothing effect of the diffusion term $(\epsilon K_{\alpha\alpha})$. Indeed, with $\epsilon = 0$, we have a pure reaction equation $K_t = -K^2$. In this case, the solution is $K(s,t) = K(s,0)/(1 + tK(s,0))$, which is singular in finite t if the initial curvature is anywhere negative. Thus, corners can form in the moving curve when $\epsilon = 0$.

As an example, consider the periodic initial cosine curve

$$\gamma(0) = (-s, [1 + \cos 2\pi s]/2) \tag{2}$$

propagating with speed $F(K) = 1 - \epsilon K$, $\epsilon > 0$. As the front moves, the troughs at $s = n + 1/2, n = 0, \pm 1, \pm 2, \ldots$. are sharpened by the negative reaction term (because $K < 0$ at such points) and smoothed by the positive diffusion term (see Figure 1a). For $\epsilon > 0$, it can be shown (see [28, 25]) that the moving front stays C^∞.

On the other hand, for $\epsilon = 0$, the front develops a sharp corner in finite time as discussed above. In general, it is not clear how to construct the normal at the corner and continue the evolution, since the derivative is not defined there. One possibility is the "swallowtail" solution formed by letting the front pass through itself (see Figure 1b). However, from a geometrical argument it seems clear that the front at time t should consist of only the set of all points located a distance t from the initial curve. (This is known as the Huygens principle construction, see [28]). Roughly speaking, we want to remove the "tail" from the "swallowtail". In Figure 1c, we show this alternate weak solution. Another way to characterize this weak solution is through the following "entropy condition" posed by Sethian (see [28]): If the front is viewed as a burning flame, then *once a particle is burnt it stays burnt.* Careful adherence to this stipulation produces the Huygens principle construction. Furthermore, this physically reasonable weak solution is the formal limit of the smooth solutions $\epsilon > 0$ as the curvature term vanishes, (see [28]).

As further illustration, we consider the case of a V-shaped front propagating normal to itself with unit speed ($F = 1$). In [27], the link between this motion and hyperbolic conservation laws is explained. If the point of the front is downwards; as the moves inwards with unit speed, a shock develops as the front pinches off, and an entropy condition is required to select the correct solution to stop the solution from being double-valued and to produce the limit of the viscous case. Conversely, if the point of the front is upwards;

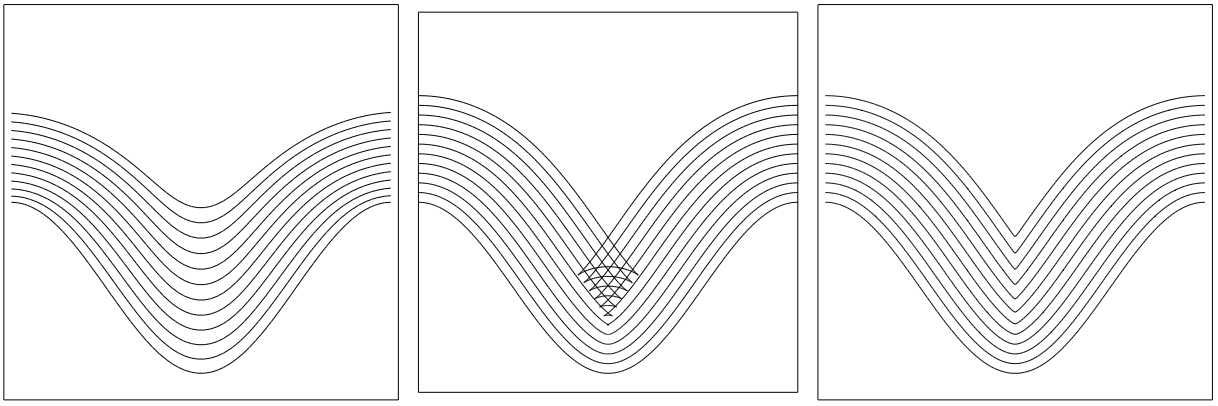

$F = 1. - 0.25K$ $Swallowtail(F = 1.0)$ $Entropy\,Satisfying(F = 1.0)$

$Fig.1a.$ $Fig.1b$ $Fig.1c$

Figure 1: Propagating Cosine Curve.

in this case the unit normal speed results in a rarefaction fan which connects the left state with slope $+1$ to the right state which has slope -1. Extensive discussion of the role of shocks and rarefactions in propagating fronts may be found in [27].

The key to constructing numerical schemes which adhere to both this entropy condition and rarefaction structure comes from the link between propagating fronts and hyperbolic conservation laws. Consider the initial front given by the graph of $f(x)$, with f and f' periodic on $[0, 1]$, and suppose that the propagating front remains a function for all time. Let ϕ be the height of the propagating function at time t, thus $\phi(x, 0) = f(x)$. The normal at (x, ϕ) is $(1, \phi_x)$, and the equation of motion becomes $\phi_t = F(K)(1 + \phi_x^2)^{1/2}$. Using the speed function $F(K) = 1 - \epsilon K$ and the formula $K = -\phi_{xx}/(1 + \phi_x^2)^{3/2}$, we get

$$\phi_t \; - \; (1 + \phi_x^2)^{1/2} = \epsilon \frac{\phi_{xx}}{1 + \phi_x^2} \tag{3}$$

Differentiating both sides of this equation yields an evolution equation for the slope $u = d\phi/dx$ of the propagating front, namely

$$u_t + [-(1 + u^2)^{1/2}]_x = \epsilon [\frac{u_x}{1 + u^2}]_x. \tag{4}$$

Thus, the derivative of the Hamilton-Jacobi equation with parabolic right-hand-side for the changing height ϕ is a viscous hyperbolic conservation law for the propagating slope u (see [30]). Our entropy condition is in fact equivalent to the one for propagating shocks in hyperbolic conservation laws. Thus, we exploit the numerical technology from hyperbolic conservation laws to build consistent, upwind schemes which select the correct entropy conditions. For details, see [25, 29].

Our goal then is to choose an appropriate speed function that yields front motion away from the body that remains smooth for all time, and thus can act to define one set of body-fit coordinate lines. Before doing so, we must extend the above ideas to include propagating fronts which are not easily written as functions. This is the level set idea introduced by Osher and Sethian [25], which we now describe.

Given a moving closed hypersurface $\Gamma(t)$, that is, $\Gamma(t=0) : [0,\infty) \to R^N$, we wish to produce an Eulerian formulation for the motion of the hypersurface propagating along its normal direction with speed F, where F can be a function of various arguments, including the curvature, normal direction, etc. The main idea is to embed this propagating interface as the zero level set of a higher dimensional function ϕ. Let $\phi(x, t=0)$, where $x \in R^N$ be defined by

$$\phi(x, t=0) = \pm d \tag{5}$$

where d is the distance from x to $\Gamma(t=0)$, and the plus (minus) sign is chosen if the point x is outside (inside) the initial hypersurface $\Gamma(t=0)$. Thus, we have an initial function $\phi(x, t=0) : R^N \to R$ with the property that

$$\Gamma(t=0) = (x | \phi(x, t=0) = 0) \tag{6}$$

Our goal is to now produce an equation for the evolving function $\phi(x,t)$ which contains the embedded motion of $\Gamma(t)$ as the level set $\phi = 0$. Let $x(t), t \in [0,\infty)$ be the path of a point on the propagating front. That is, $x(t=0)$ is a point on the initial front $\Gamma(t=0)$, and $x_t = F(x(t))$ with the vector x_t normal to the front at $x(t)$. Since the evolving function ϕ is always zero on the propagating hypersurface, we must have

$$\phi(x(t), t) = 0 \tag{7}$$

By the chain rule,

$$\phi_t + \nabla\phi(x(t,t)) \cdot x'(t) = 0 \tag{8}$$

Since F already gives the speed in the outward normal direction, then $x'(t) \cdot n = F$ where $n = \nabla\phi / |\nabla\phi|$. Thus, we then have the evolution equation for ϕ, namely

$$\phi_t + F|\nabla\phi| = 0 \tag{9}$$

$$\phi(x, t=0) \quad given \tag{10}$$

We refer to this as a Hamilton-Jacobi "type" equation because, for certain forms of the speed function F, we obtain the standard Hamilton-Jacobi equation.

In Figure 2, (taken from [31]), we show the outward propagation of an initial curve and the accompanying motion of the level set function ϕ. In Figure 2a, we show the initial circle, and in Figure 2b, we show the circle at a later time. In Figure 2c, we show the initial position of the level set function ϕ, and in Figure 2d, we show this function at a later time.

There are four major advantages to this Eulerian Hamilton-Jacobi formulation. The first is that the evolving function $\phi(x,t)$ always remains a function as long as F is smooth. However, the level surface $\phi = 0$, and hence the propagating hypersurface $\Gamma(t)$, may change topology, break, merge, and form sharp corners as the function ϕ evolves, see [25].

The second major advantage of this Eulerian formulation concerns numerical approximation. Because $\phi(x,t)$ remains a function as it evolves, we may use a discrete grid in the domain of x and substitute finite difference approximations for the spatial and temporal derivatives. For example, using a uniform mesh of spacing h, with grid nodes (i,j), and employing the standard notation that ϕ_{ij}^n is the approximation to the solution $\phi(ih, jh, n\Delta t)$, where Δt is the time step, we might write

$$\frac{\phi_{ij}^{n+1} - \phi_{ij}^n}{\Delta t} + (F)(\nabla_{ij}\phi_{ij}^n) = 0 \tag{11}$$

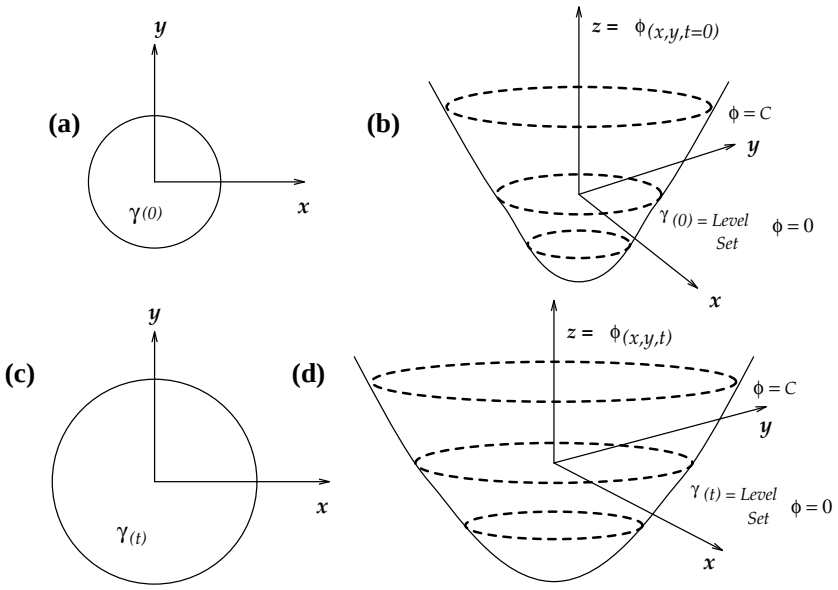

Figure 2: Propagating Circle

Here, we have used forward differences in time, and let $\nabla_{ij}\phi_{ij}^n$ be some appropriate finite difference operator for the spatial derivative. As discussed above, the correct entropy-satisfying approximation to the difference operator comes from exploiting the technology of hyperbolic conservation laws. Following [25], given a speed function $F(K)$, we update the front by the following scheme. First, separate $F(K)$ into a constant advection term F_0 and the remainder $F_1(K)$, that is,

$$F(K) = F_0 + F_1(K) \tag{12}$$

The advection component F_0 of the speed function is then approximated using upwind schemes, while the remainder is approximated using central differences. In one space dimension with $F_0 positive$, we have

$$\phi_i^{n+1} = \phi_i^n - \Delta t F_0 \left[\left(\max(D_i^-, 0)^2 + \min(D_{i,0}^+)^2 \right)^{1/2} - |F_1(K) \nabla \phi_i^n| \right] \tag{13}$$

Extension to higher dimensions are straightforward; we use the version introduced in [33].

The third major advantage of the above formulation is that intrinsic geometric properties of the front may be easily determined from the level function ϕ. For example, at any point of the front, the normal vector is given by

$$\vec{n} = \frac{\nabla \phi}{|\nabla \phi|} \tag{14}$$

and the curvature is easily obtained from the divergence of the gradient of the unit normal vector to front, i.e.,

$$K = \nabla \cdot \frac{\nabla \phi}{|\nabla \phi|} = -\frac{\phi_{xx}\phi_y^2 - 2\phi_x \phi_y \phi_{xy} + \phi_{yy}\phi_x^2}{(\phi_x^2 + \phi_y^2)^{3/2}} \tag{15}$$

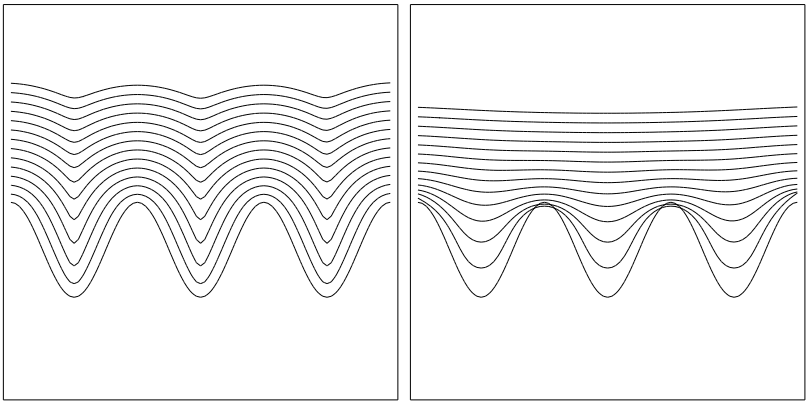

$F = 1. - 0.025K$ $F = 1. - 0.25K$

Fig.3a. *Fig.3b*

Figure 3: Propagating Triple Sine Curve.

Finally, the fourth major advantage of the above level set approach is that there are no significant differences in following fronts in three space dimensions. By simply extending the array structures and gradient operators, propagating surfaces are easily handled.

As an example of the application of level set methods, consider once again the problem of a front propagating with speed $F(K) = 1 - \epsilon K$. In Figure 3, we show two cases of a propagating initial triple sin curve. For ϵ small (Fig. 3a), the troughs sharpen up and will result in transverse lines that come too close together. For ϵ large (Fig. 3b), parts of the boundary with high values of positive curvature can initially move inwards, and concave parts of the front can move quickly up.

3 Extensions of the Level Set Technique

3.1 Fast Level Set Methods

The main issue in the level set approach is the extension of the speed function F to all of space in order to move all the level sets, not simply the zero level set on which the speed function is naturally defined. While this may be straightforward in some cases, it is not efficient, since one must perform considerable computational labor away from the front to advance the other level sets.

In [1], an approach introduced by Chopp in [10] and used in recovering images in [23], was refined and analyzed extensively. The central idea is to focus computational effort in a narrow band about the zero level set. We only update the values of the level set function ϕ in this thin zone around the interface. Thus, in two dimensions, an $O(N^2)$ calculation, where N is the number of grid points per side, reduces to an $O(kN)$ calculation, where k is the number of cells in the narrow band. This reduction of labor makes the method typically much faster than marker particle methods, due to the need for many marker points per mesh cell in order to obtain acceptable accuracy. As the front moves, the narrow band must occasionally be rebuilt (known as "re-initialization") of the interface. For details, see [10, 23, 1].

Scheme	40 Cells	80 Cells	16 Cells
Narrow Band 1st Order	125.1	243.5	507.9
Full Matrix 1st Order	330.9	1367.5	5657.6
Narrow Band 2nd Order	118.8	250.5	547.8

Figure 4: Comparative Timings of Schemes

Briefly, the entire two-dimensional grid of data is stored in a square array. A one–dimensional object is used to keep track of which points in this array correspond to the tube, and the values of ϕ at those points are updated. When the front moves half the distance towards the edge of the tube boundary, the calculation is stopped, and a new tube is built with the zero level set interface boundary at the center. Details on the accuracy, typical tube sizes, and number of times a tube must be rebuilt may be found in [1].

As an example of the speed up possible using this approach, we cite the results given in [1]. On a typical two-dimensional interface tracking problem, we compare timings of a first and second order narrow band approach with the the full matrix approach; calculations are performed over various grid sizes. Results are measured in a rough manner, with optimization turned off and timing compared using the Unix time command. Thus, the important feature are the ratios. The narrow band calculation is around 10 times faster for the finest calculation than the full matrix solution.

3.2 Multiple Interfaces and Triple Point Junctions

As initially designed in [25], the level set technique is designed to track an interface where there is a clear distinction between an "inside" and "outside". This is because the interface is assigned the zero level value between the two regions. Some work has been done on extending the approach to multiple fluids; mostly notably in [5] where an extensive study of the motion of triple points was made. In the approach presented there, at each time step the calculation stops, the zero level set is found, and the entire level set function is rebuilt using a reinitialization technique.

In many cases, such an approach is not necessary; in [34] a level approach is given for tracking an arbitrary number of interfaces in two and three dimensions which includes the motion of triple points in some cases. The technique presented does not rely on any reinitialization, and retains the essential characteristic of the original approach; the front is only explicitly constructed for display purposes. Here, we briefly review the approach, for details, see [34].

The key idea lies in recasting the interface motion as the motion of one level set function for each material. In some sense, this is what was done in the re-ignition idea given in [26]. In that approach, the front was a flame which propagated downstream under a fluid flow, and was re-ignited at each time step at a flame holder point. This "re-ignition" was executed by taking the minimum of the advancing flame and its original configuration around the flame holder, thus ensuring that the maximum burned fluid is achieved.

Imagine that we have N separate regions, and a full set of all possible pairwise speed functions F_{IJ} which describe the propagation speed of region I into region J; F is taken as zero if Region I cannot penetrate J. The idea is to advance each interface to obtain a trial value for each interface with respect to motion into every other region, and then combine the trial values in such a way as to obtain the maximum possible motion of the interface.

In general then, we proceed as follows. Given a Region I, we obtain $N-1$ trial level set functions ϕ^*_{IJ}

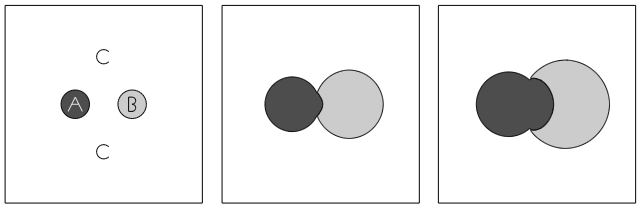

Fig.5a *Fig.5b* *Fig.5c*

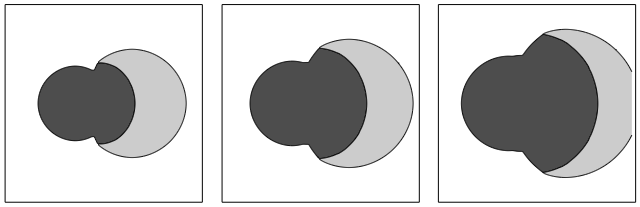

Fig.5d *Fig.5e* *Fig.5f*

Influence Matrix	on A	on B	on C
Effect of A	1.0	3.0	1.0
Effect of B	0.0	1.0	2.0
Effect of C	0.0	0.0	1.0

Figure 5: A into C with speed 1, A into B with speed 3, B into C with speed 2

by moving the Region I into each possible Region J, J=1,N ($J \neq I$) with speed F_{IJ}. During the motion of Region I into Region J, we assume that all other regions are impenetrable. We then test the penetrability of the Region J itself, leaving the value of ϕ^*_{IJ} unchanged if $F_{IJ} \neq 0$, else modifying it with the maximum of itself and $-\phi^*_{JI}$. Finally, to allow Region I to evolve as much as possible, we take the minimum over all possible motions to obtain the new position; this is the re-ignition idea described earlier. Complete details of the approach may be found in [34].

As illustration of our approach, we show two examples. First, we show three regions, described as Regions A, B, and C. Region A grows with speed 1 into Region C, and Region B grows with speed 2. Once they come into contact, Region A dominates Region B with speed 3, thus Region B grows through Figure 5c, and then is "eaten up" by the advancing Region A. Note what happens; Region A advances with speed 3 to the edge of Region B, which is only advancing with speed 1 into Region C. However, Region A cannot pass Region B, because *its* speed into Region C is slower than that of Region B.

Next, we study the motion of a triple point between Regions A, B, and C. We assume that Region A penetrates B with speed 1, B penetrates C with speed 1, and C penetrates A with speed 1. The exact solution to this is given by a spiral with no limiting tangent angle as the triple point is approached. The triple point does not move; instead, the regions spiral around it. In Figure 6, we show the results calculated on a 98x98 grid. Starting from the initial configuration, the regions spiral around each other, with the leading tip of each spiral controlled by the grid size. In other words, we are unable to resolve spirals tighter than the grid size, and hence that controls the fine scale description of the motion. However, we note that the triple point remains fixed.

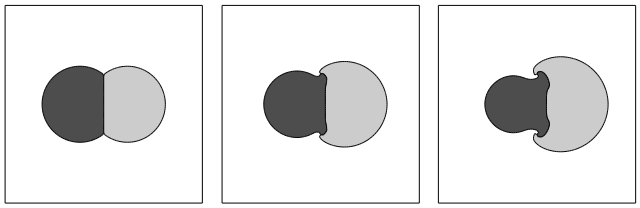

$Fig.6a\ T = 0.0$ $Fig.6b\ T = 1.0$ $Fig.6c\ T = 2.0$

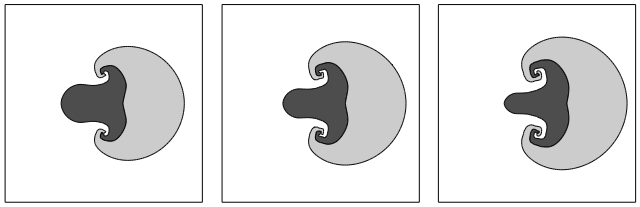

$Fig.6d\ T = 3.0$ $Fig.6e\ T = 4.0$ $Fig.6f\ T = 5.0$

Influence Matrix	on A	on B	on C
Effect of A	1.0	1.0	0.0
Effect of B	0.0	1.0	1.0
Effect of C	1.0	0.0	1.0

Figure 6: Spiraling Triple Point: 98x98 Grid

3.3 Fast Reinitialization Techniques

There are two situations in which rebuilding the signed distance level set function, or "reinitialization" may be required. The first is in the narrow band technique, in which once the front leaves the narrow band a new band must be constructed. The second is in situations in which the velocity of the interface corresponding to the zero level does not extend naturally to the other level sets, or gives rise to complex motion of the other level sets. The issue was first discussed in [24], in which the use of the level set method to perform image segmentation led to an image-based speed term which had no meaning for any other contour besides the interface itself. Another example of this problem is in simulations of the motion of a fluid boundary between two fluids with large density differences. While the fluid velocity is a natural candidate for the speed function of all the level sets, it is easy to see that this is a poor choice; the fluid velocity in the lighter fluid can be orders of magnitude larger than that in the heavier fluid, giving rise to wild gradients in the level set motions of contours neighboring the zero level set. Consequently, one is faced with two approaches. The first approach is devise an extension speed function which, although having no real physical meaning away from the interface itself, behaves appropriately for the other level sets and has the correcting limiting value on the zero level set. This is the approach taken in [33]. The second approach is to simply use any convenient velocity field (for example, the fluid velocity in the two-fluid problem), and then re-initialize the level set function periodically to rebuild the level sets around the position of the zero level set.

This is the approach taken in [10], in which the level set function is rebuilt in a small band about the front by first finding the front explicitely and then recomputing the signed distance from this front at all grid points in the narrow band around the front. An alternative technique was introduced and employed in

[9]; in that work, the level set function was rebuilt by solving the associated equation

$$\phi_t = S(\phi)(1 - |\nabla\phi|) \tag{16}$$

where $S(\phi)$ is the sign of ϕ. By solving this equation until steady-state convergence, the left hand side becomes zero and the resulting value of $\nabla\phi$ becomes one, which corresponds to a initialization of ϕ by the distance function.

This technique can be made efficient; however, since the switch function given by $S(\phi)$ only chooses direction on the basis of values on the grid, much of the sub-grid information about the location of the interface is lost. This is because the use of the sign function pays no attention to the actual location of the zero level set within a particular cell, which can be seen by considering a simple one-dimensional example.

Instead, we use an alternate technique, first discussed in [31], described in [34], and used extensively in [2, 3]. Suppose that at some time one has a level set function ϕ whose zero level set corresponds to the position of the interface. The goal is to rebuild the level set function without disturbing the zero level set so that the new function corresponds to the signed distance function. We do this as follows. First, flow the level set function forward in time with speed function $F = 1$, and measure the time when the value of ϕ at each grid point ahead of the front (that is, for all values of $\phi > 0$) changes sign. The time when the sign changes clearly corresponds to the distance to the front by Huyghen's principle, see [28]. Second, repeat the process by flowing the front backwards, that is, with speed $F = -1$ and again compute the zero crossing time.

This procedure results in a highly accurate rebuilding of the signed distance function around the zero level set corresponding to the interface. It can be performed using a high order method, and is extremely fast if one chooses a large time step near the edge of the Courant condition. We use it in all level set methods required reinitialization. For details, see [34].

4 Interface Problems in CFD and Material Science

In this section, we discuss some recent applications of the level set technique to a variety of problems in CFD and material processing.

4.1 Generation of Body-fitted Logically Rectangular Grids

The generation of logically rectangular grids around and inside complex bodies is still an art. While unstructured meshes may be obtained in a relatively automated fashion, many calculations require the accuracy of a logically rectangular, body-fitted grid. For example, high Reynolds turbulent flow requires an accurate, body-fit grid in the boundary layer where gradients are steep and a highly accurate scheme is critical. Standard techniques in logical rectangular boundary-fitted grid generation fall under four general categories. Hyperbolic grids march out from the boundary. Algebraic grids adjust nodes until a desired shape is achieved. Elliptic grids solve an associated elliptic partial differential equation,and variational methods minimize certain functionals. Grids obtained through these techniques can be plagued by colliding grid lines, inability to handle sharp corners in the bodies, and difficulty extending to three space dimensions.

Recently, level set techniques have been applied to grid generation in two and three dimensions, [31]. Here, we review some of that work; for details see [31].The technique hinges on viewing the boundary of the body as a propagating front. The front is then allowed to propagate with a speed law that ensures that it

will smoothly evolve from the body in such a way that the position of the front yields one set of coordinate lines. The judicious choice of speed function produces a geometry-flowing interface which is guaranteed to handle cusps and corners, produce smooth contours, and trivially extend to three space dimensions. Lines orthonormal to the propagating, body-fitted, level-set lines are obtained by following the trajectories of particles propagating with a speed function dependent on the local curvature and emanating from the boundary.

Using this approach, the resulting algorithm generates two and three dimensional interior and exterior grids around reasonably complex bodies which may contain sharp corners and significant variations in curvature. We have also used these techniques to produce non-uniform solution-adaptive meshes and boundary-fitted moving grids. The algorithm is completely automatic; the only user-supplied grid-dependent parameters are the shape of the initial boundary, and the time step spacing for the evolving front function. In Figure 7, we show the results of this application. In Figure 7a, a two-dimensional external grid is produced around a fairly complex object; in Figure 7b, an internal grid is computed. Finally, in Figure 7c, a three-dimensional grid is obtained. In the exterior grid cases, a speed function was chosen of the generic form $1 - \epsilon K$, where K is the curvature; in the case of the interior grid, the speed function was chosen as $F = \min(\delta, K)$, where δ is a threshold value chosen to ensure that every point of the body moves inwards with some minimum speed. Without such a factor, points on non-convex boundaries would first evolve outwards at some points, which violates the ability of the algorithm to create a grid.

The above approach is automatic, inexpensive, and requires no complex alteration in three-dimensions. To extend it to multiple bodies, current work is aimed at using the above level set approach to grid generation to generate a logically rectangular grid near each body (for example, in the boundary layer and past), and then take these grids as input to more traditional techniques which can grid multiple bodies, but cannot access complex shapes in an automatic fashion. Thus, the approach is a marriage of the level set algorithm to generate an accurate near-body grid which yields a smoother, almost convex shape, and a traditional methodology which will patch these smooth grids together. For details of this approach, see [32].

4.2 Flame Propagation and Combustion

Level set methods have been used to track combustion and flame fronts; here, we report on two such calculations. First, in [26], the method is used to the study the stability of a flame attached to a flame holder. Here, the effects of upstream turbulence, exothermic effects due to volume expansion along the flame front, flame speed dependence on curvature, and vorticity production along the flame front due to the baroclinic term as manifested through flame stretch are all considered. The model uses the level set method to track the position and curvature of the evolving flame, producing internal boundary conditions for the flame-induced exothermic and baroclinic velocity fields. In Figure 8 we show two effects; first, in Fig.8a, taken from [26], an incoming upstream turbulence field interacts with exothermic production along the flame front. Successive time photos are superimposed, showing the width of flame brush. In Fig.8b, the effects of vorticity production along the flame front is added; in this case, the incoming turbulence field stretchs and contorts the flame which then causes flame stretch, inducing vorticity which self-wrinkles the flame. This effect is seen in the widening of the flame brush.

Next, we show the results of simulations in [36], in which a level set method to track combustion regions is coupled to a projection method for the incompressible flow field. In Figure 9, taken from [36], we show ignition at the center of a doubly periodic shear jet; the flame propagates with a speed that depends on the local curvature. The results show the ability of the level set method to follow sharp corners, track cusps,

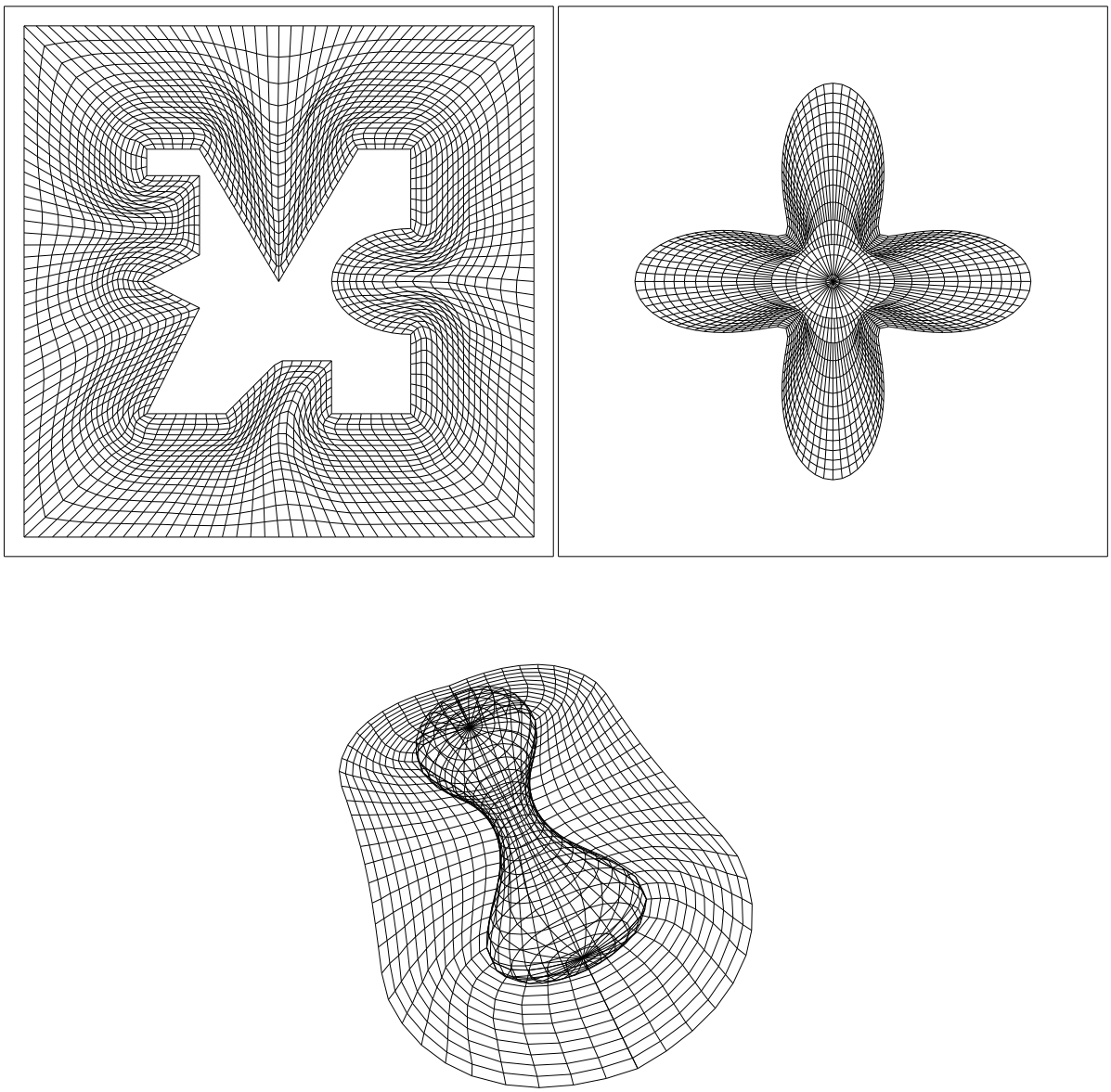

Figure 7: Level Set Approach to Grid Generation

Exothermic Only *Exothermicity and Baroclinicity*

Figure 8: Stability of Flame Under Exothermic and Baroclinic Effects

and change topology.

4.3 Crystal Growth and Dendritic Solidification

In [33], level set methods were used to compute the motion of complex solid/liquid boundaries in crystal growth. The model includes physical effects such as crystalline anisotropy, surface tension, molecular kinetics and undercooling. The fundamental coupling is due to a single history-dependent boundary integral equation on the solid/liquid boundary developed by Strain [35]. The setup of the problem is as follows; a supercooled liquid is placed within a container, and a small solid seed disturbance is placed in the center. This initiates a rapid and unstable dendritic solidification problem, in which the solid phase sends branching fingers into the distant cooler liquid near the undercooled walls. Hence the problem becomes a moving boundary problem, in which the temperature field satisfies a heat equation in each phase, coupled through two boundary conditions on the unknown moving solid/liquid boundary, as well as initial and boundary conditions.

Numerical experiments were performed in [33] by coupling the level set method to the boundary integral formulation, and showed the evolution of complicated shapes with spikes and corners, topological changes in the solid-liquid boundary, dendrite formation and sidebranching. In Figure 10, we show the results of one such calculation, obtained by slowing increasing the latent heat of formation. The results show that as this term is increased, the front becomes markedly unstable as it is drawn to the side walls, and produces significant side-branching and tip splitting.

4.4 Microfabrication of Electronic Components: Etching, Deposition, and Lithography

Finally, we show the application of level set techniques to problems in etching, deposition and photolithography, which are occur in the manufacture of electronic components. In [2, 3], the effects of three dimensional etching and deposition under the effects of visibility, directional, and source flux functions, evolution of

Figure 9: Combustion in Doubly-Periodic Shear Layer

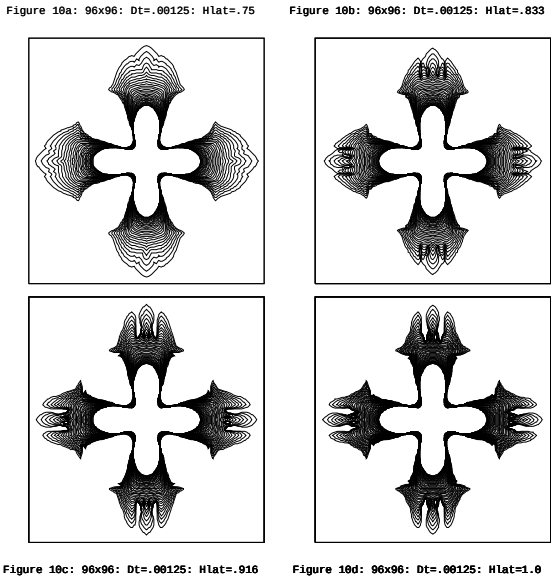

Figure 10: Effects of Latent Heat on Dendritic Growth in Solidification

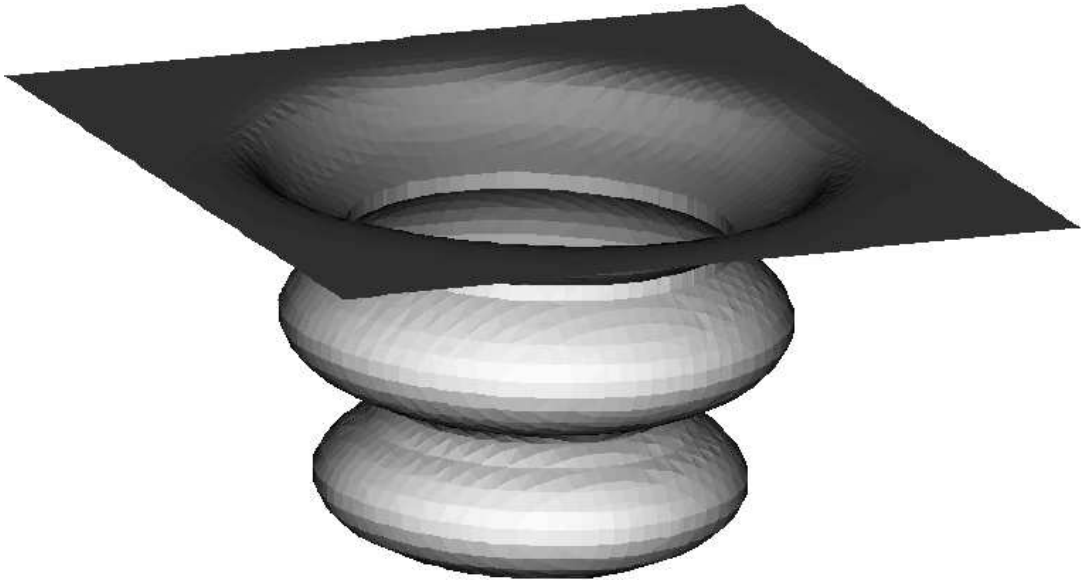

Figure 11: Profile Obtained under Photolithography

lithographic profiles, discontinuous etch rates through multiple materials, and non-convex sputter yield flux functions are considered.

In this application, the goal is to follow the evolution of a material surface profile under the effects of:

- *Deposition:* in which particles are deposited on the surface, causing build-up in the profile, either through isotropic ("wet" deposition) or under directional deposition,
- *Etching:* Particles remove material from the evolving profile boundary. The material may be isotropically removed, known again as chemical or "wet" etching, or chipped away through reactive ion etching, also known as "ion milling",
- *Lithography:* in which the underlying material is treated by an electromagnetic wave which alters the resist property of the material.

We show the results of two simulations. First, in Figure 11, we show the three-dimensional resist surface obtained under a rate function obtained through a bleach process. The level set method tracks the undulations in the evolving profile driven by the underlying standing electromagnetic wave.

Finally, in Figure12, we show results of a saddle surface being etched away under a non-convex sputter etch law of the form $F = [1 + 4\sin^2(\theta)]\cos(\theta)$ where θ meaures the angle between the surface normal and the vertical direction. This motion gives rise to faceting at corners and unusual rarefaction structures. Such a speed law is used in sputter etching, in which enhanced directionality is desired.

Acknowledgements: All calculations were performed at the University of California at Berkeley and the Lawrence Berkeley Laboratory.

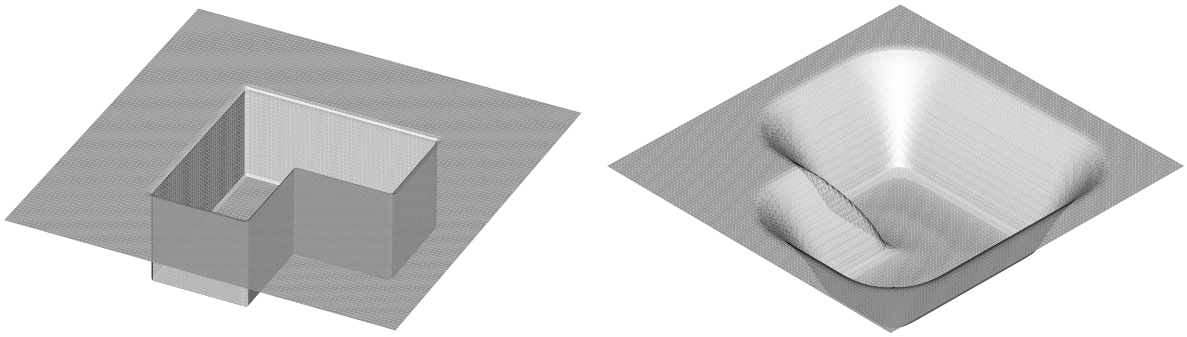

$Initial \quad Shape : T = 0$ $\qquad\qquad$ $F = [1 + 4\sin^2(\theta)]\cos(\theta) \quad T = 8(rotated)$

Figure 12: Saddle Surface Under Non-Convex Directional Sputter Etch

References

[1] Adalsteinsson, D., and Sethian, J.A., *A fast level set method for propagating interfaces*, to appear, Jour. Comp. Phys., 1995.

[2] Adalsteinsson, D., and Sethian, J.A., *A Level Set Approach to a Unified Model for Etching, Deposition, and Lithography I: Algorithms and Two-Dimensional Simulations*, to appear, J. Comp. Phys., 1995.

[3] Adalsteinsson, D., and Sethian, J.A., *A Level Set Approach to a Unified Model for Etching, Deposition, and Lithography II: Three-Dimensional Simulations*, submitted for publication, J. Comp. Phys., March 1995.

[4] Altshuler, S., Angenent, S.B., and Giga, Y., *Mean Curvature Flow through Singularities for Surfaces of Rotation*, preprint, 1993.

[5] Merriman, B., Bence, J., and Osher, S.J., *Motion of Multiple Junctions: A Level Set Approach*, to appear, Jour. Comp. Phys., 1994.

[6] Bourlioux, A., and Sethian, J.A., *A Conservative Level Set Method for Fluid Interfaces*, to be submitted, 1994.

[7] Casselles, V., Catte, F., Coll, T., and Dibos, F., *A Geometric Model for Active Contours*, Numerische Mathematic, Vol. 60, pp. 1-31, 1993.

[8] Chen, Y., Giga, Y., and Goto, S., *Uniqueness and Existence of Viscosity Solutions of Generalized Mean Curvature Flow Equations*, J. Diff. Geom, Vol. 33, 749, 1991.

[9] Chang, Y.C., Hou, T.Y., Merriman, B., and Osher, S.J., *A Level Set Formulation of Eulerian Interface Capturing Methods for Incompressible Fluid Flows*, submitted for publication, Jour. Comp. Phys., 1994.

[10] Chopp, D. L., *Computing minimal surfaces via level set curvature flow*, Journal of Computational Physics, Vol. 106, pp. 77–91, 1993.

[11] Chopp, D. L., *Construction of Self-Similar Surfaces* Need reference, 1994.

[12] Chopp, D.L. and Sethian, J.A., *Flow under Curvature: Singularity Formation, Minimal Surfaces, and Geodesics*, to appear, Jour. Exper. Math, 1994.

[13] Evans, L.C., Sonar, H.M., and Souganidis, P.E., *Phase Transitions and Generalized Motion by Mean Curvature*, Communications on Pure and Applied Mathematics, Vol. 45, 1097, 1992.

[14] Evans, L.C., and Spruck, J., *Motion of Level sets by Mean Curvature*, J. Diff. Geom, Vol. 33, pp. 635-681, 1991.

[15] Evans, L.C., and Spruck, J., *Motion of Level sets by Mean Curvature II*, Transactions of the American Mathematical Society, Vol. 330, 91, 1992.

[16] Falcone, M., Giorgi, T., and Loretti, P., *Level Sets of Viscosity Solutions and Applications*, Instituto per le Applicazioni del Calcolo, Rome, preprint, 1990.

[17] Gage, M., *Curve Shortening Makes Convex Curves Circular*, Inventiones Mathematica, Vol. 76, 357, 1984.

[18] Gage, M., and Hamilton, R., *The Equation Shrinking Convex Planes Curves*, J. Diff. Geom, Vol. 23, 69, 1986.

[19] Giga, Y., and Goto, S., *Motion of Hypersurfaces and Geometric Equations*, Journal of the Mathematical Society of Japan, Vol. 44, 99, 1992.

[20] Grayson, M., *The heat equation shrinks embedded plane curves to round points*, J. Diff. Geom., Vol. 26, 285 (1987).

[21] Huisken, G., *Flow by mean curvature of convex surfaces into spheres*, J. Diff. Geom., Vol. 20, 237, (1984).

[22] Kimmel, R., and Bruckstein, A., *Shape from Shading via Level Sets*, Center for Intelligent Systems Report No.9209, Technion- Israel Institute of Technology, June 1992,

[23] Malladi, R., Sethian, J. A., and Vemuri, B. C., *Shape modeling with front propagation: A level set approach*, Center for Pure and Applied Mathematics, Report PAM-589, Univ. of California, Berkeley, August 1993.

[24] Malladi, R., Sethian, J.A., *A Unified Framework for Shape Segmentation, Representation, and Recognition*, submitted August 1994, CVGIP - Image Understanding.

[25] Osher, S., and Sethian, J. A., *Fronts propagating with curvature dependent speed: Algorithms based on Hamilton-Jacobi formulation*, Jour. Comp. Phys., Vol. 79, pp. 12-49, 1988.

[26] Rhee, C., Talbot, L. and Sethian, J.A., *Dynamical Study of a Premixed V Flame*, Submitted for Publication, Jour. Fluid Mech. 1994.

[27] Sethian, J.A., *An Analysis of Flame Propagation*, Ph.D. Dissertation, Mathematics, University of California, Berkeley, 1982.

[28] Sethian, J.A., *Curvature and the evolution of fronts*, Commun. in Math. Physics, Vol. 101, pp. 487–499, 1985.

[29] Sethian, J.A., *Numerical algorithms for propagating interfaces: Hamilton-Jacobi equations and conservation laws*, Jour. of Diff. Geom., Vol. 31, pp. 131-161, 1990.

[30] Sethian, J.A., *Numerical methods for propagating fronts*, in Variational methods for free surface interfaces, edited by P. Concus and R. Finn, (Springer-Verlag, New Work, 1987).

[31] Sethian, J.A., *Curvature Flow and Entropy Conditions Applied to Grid Generation*, to appear, J. Comp. Phys. 1994.

[32] Sethian, J.A., *Three-Dimensional Grid Generation Using Curvature Flow and Level Sets.* work in progress.

[33] Sethian, J.A. and Strain, J.D., *Crystal Growth and Dendritic Solidification* J. Comp. Phys., Vol. 98, pp. 231-253, (1992).

[34] Sethian, J.A., *Tracking the Evolution of Multiple Interfaces and Multi-Junctions* submitted for publication, 1995, J. Comp. Phys.

[35] Strain, J., *A Boundary Integral Approach to Unstable Solidification*, J. Comp. Phys., Vol. 85, pp. 342-389, (1989).

[36] Zhu, J. and Sethian, J.A., *Projection Methods Coupled to Level Set Interface Techniques* J. Comp. Phys., Vol. 102, pp.128-138, 1992.